

# SIAE-Mediated Loss of Sialic Acid Acetylation Contributes to Ulcerative Colitis

Siyue Bo<sup>1,\*</sup>, Xiaotong Wang<sup>1-3,\*</sup>, Jiani Qian<sup>1,4</sup>, Guoqiang Ma<sup>5</sup>, Zheng Ying<sup>5</sup>, Duanmin Hu<sup>2</sup>, Chunyan Hou<sup>6</sup>, Junfeng Ma<sup>6</sup>, Longjiang Xu<sup>4</sup>, Shuang Yang<sup>1,7,8</sup>

<sup>1</sup>Center for Clinical Mass Spectrometry, College of Pharmaceutical Sciences, Soochow University, Suzhou, Jiangsu, 215123, People's Republic of China;

<sup>2</sup>Department of Gastroenterology, The Second Affiliated Hospital of Soochow University, Suzhou, Jiangsu, 215004, People's Republic of China;

<sup>3</sup>Department of Hepatology and Gastroenterology, The Affiliated Infectious Hospital of Soochow University, Suzhou, 215004, People's Republic of China; <sup>4</sup>Department of Pathology, The Second Affiliated Hospital of Soochow University, Suzhou, Jiangsu, 215000, People's Republic of China; <sup>5</sup>Jiangsu Key Laboratory of Neuropsychiatric Diseases, College of Pharmaceutical Sciences, Soochow University, Suzhou, Jiangsu, 215123, People's Republic of China; <sup>6</sup>Department of Oncology, Lombardi Comprehensive Cancer Center, Georgetown University Medical Center, Georgetown University, Washington, DC, 20057, USA; <sup>7</sup>Department of Respiratory Medicine, The Fourth Affiliated Hospital of Soochow University, Suzhou, Jiangsu, 215123, People's Republic of China; <sup>8</sup>Health Management Center, the second Affiliated Hospital of Soochow University, Suzhou, People's Republic of China

\*These authors contributed equally to this work

Correspondence: Shuang Yang; Longjiang Xu, Email yangs2020@suda.edu.cn; szdocxu@suda.edu.cn

**Background:** Ulcerative colitis (UC) disrupts the colon's protective mucus layer, exposing the epithelium to bacteria and triggering inflammation. This barrier, crucial for intestinal health, depends on complex glycosylation, notably sialic acid modifications. However, the precise role of sialic acid acetylation and the enzyme SIAE (sialic acid acetyltransferase) in UC pathogenesis remains unclear. This study investigates the role of glycosylation changes, specifically sialic acid de-acetylation, in UC progression.

**Methods:** Tissue samples were obtained from patients with ulcerative colitis (UC) and colorectal cancer at the Second Affiliated Hospital of Soochow University. HT-29 cells were utilized to investigate the molecular mechanisms of SIAE in UC pathogenesis. Mass spectrometry was performed to analyze differences in protein and glycoprotein expression. Western blot (WB) and immunohistochemistry (IHC) were used to examine SIAE protein expression changes during inflammation. Furthermore, polymerase chain reaction (PCR) and immunofluorescence were employed to determine the effects of SIAE on sialic acid levels and mucosal immunity.

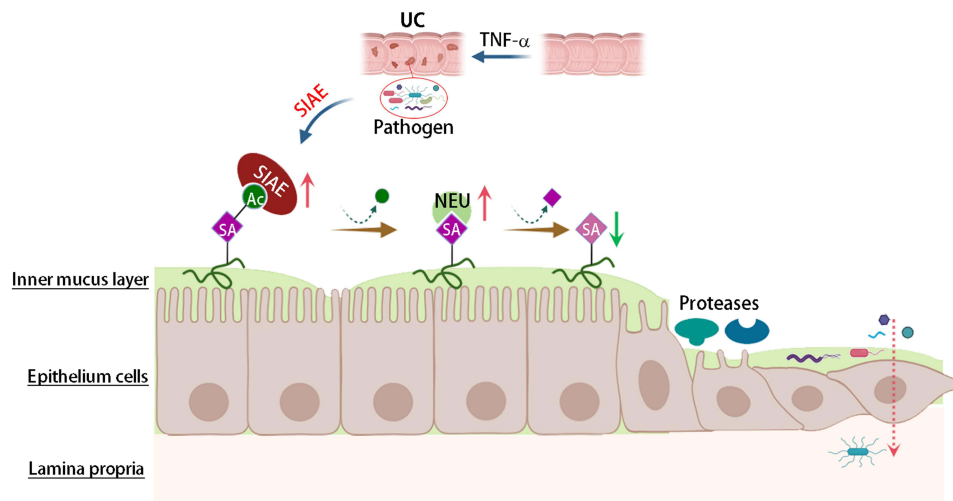
**Results:** In this study, we characterized proteins and glycoproteins from patient tissues with UC, finding that sialic acid acetyltransferase (SIAE) is upregulated in UC. HT-29 cells exposed to TNF- $\alpha$  induced an inflammatory response with a 5-fold increased expression of SIAE and NEU1 when TNF- $\alpha$  was at a concentration of 100 ng/mL. Mass spectrometry analysis revealed a reduction in acetylation on glycans and glycoproteins, while confocal microscopy confirmed a decrease in sialic acid on the cell surface. Gene expression analysis showed that *CDH1*, *CTNND1*, and *ITGA8* were significantly downregulated in HT-29 cells stimulated by TNF- $\alpha$ , suggesting a reduction in cell-cell adhesion. SNA lectin-confocal microscopy revealed a reduction of sialic acid on HT-29 cells in TNF- $\alpha$ -induced UC cell models.

**Conclusion:** This study demonstrates that SIAE is significantly upregulated in ulcerative colitis (UC) tissues and TNF- $\alpha$ -stimulated HT-29 cells, leading to a marked reduction in sialic acid acetylation and cell surface sialic acid levels. These changes correlate with decreased expression of cell adhesion molecules, suggesting a disruption of the mucosal barrier integrity. Consequently, SIAE-mediated sialic acid de-acetylation emerges as a critical factor in UC pathogenesis, potentially serving as both a valuable biomarker and a promising therapeutic target.

**Plain Language Summary:** Ulcerative colitis (UC) is a disease where the lining of the large intestine becomes inflamed. This inflammation can damage the protective mucus layer, allowing bacteria to enter and trigger more inflammation. In this study, researchers found that a protein called SIAE is increased in UC patients. This protein breaks down sialic acid, a sugar molecule that helps protect the lining. When sialic acid levels decrease, the protective barrier weakens, leading to more inflammation and potentially worsening UC.

**Keywords:** glycan, sialic acid, sialic acid acetyltransferase, ulcerative colitis, inflammation bowel disease, mass spectrometry

## Graphical Abstract



## Introduction

Inflammatory bowel disease (IBD) is a chronic condition that requires patients to manage for the rest of their life. It has over 6.8 million cases worldwide, with an incidence of 10.9 per 100,000 in the United States.<sup>1,2</sup> The exact cause of IBD remains unknown, but it is believed to be a complex interplay of genetic and environmental factors. Population-based studies have demonstrated evidence that genetic factors can contribute to the pathogenesis of IBD, with an approximate 8- to 10-fold greater risk of developing IBD in individuals whose relatives have ulcerative colitis (UC) or Crohn's disease (CD).<sup>3,4</sup> An overactive immune system, possibly triggered by certain genetic and environmental factors like diet, stress, or infections, mistakenly attacks healthy gut tissue. Studies have shown that genetic loss of a cytokine such as interleukin-10 (IL-10) or its receptor can lead to early-onset IBD in infants and children.<sup>5</sup> Conversely, non-genetic factors such as smoking, vaccinations, and antibiotics have been implicated in the increased incidence of IBD.<sup>6</sup> Therefore, understanding the mechanism of IBD can provide an effective therapeutic strategy for drug development and treatment.

Ulcerative colitis (UC) is the most common type of IBD, affecting the rectum and colon to a variable extent, with 5 million cases globally in 2023.<sup>7</sup> Common symptoms include persistent diarrhea, rectal bleeding, abdominal pain, urgency to defecate, fatigue, and anemia.<sup>8</sup> UC typically starts in the rectum and can spread continuously up the colon, forming open sores on the inflamed lining of the colon. The thinner colon lining directly relates to a damaged mucous layer, primarily composed of mucins produced by goblet cells, and compromised epithelial cell adhesion. Studies have shown that the depleted mucosal barrier is one of the primary abnormalities in pediatric UC, where bacteria coated with IgA and IgG can penetrate the mucin layer.<sup>9</sup> MUC2 is the major component of the colon mucus layer, with less expressed proteins such as IgG Fc-binding protein (FCGBP), chloride channel (CLCA1, CLCA3), zymogen granule protein 16 (ZG16), anterior gradient protein 2 homolog (AGR2), and immunoglobulins. The outer mucus layer serves as a regulator of host-microbial interactions, while the inner layer is much denser to prevent bacteria from penetrating the epithelium.<sup>10</sup> The gel-like MUC2 mucin carries enormous O-glycans that selectively interact with the gut microbiota to colonize beneficial bacteria while preventing harmful ones.<sup>11</sup> Thus, altered MUC2 O-glycans can degrade its defense ability, as truncated O-glycans, especially core 3, are observed in UC patients.<sup>12</sup> This study investigates how glycosylation changes, specifically sialic acid de-acetylation, contribute to UC progression.

Sialylation of mucus proteins is significantly altered in the mucus layer of UC patients. Early research found an increased rate of sialylation of colonic mucin using mucosal explants from UC tissues, measured by the incorporation of *N*-acetylmannosamine (ManNAc) into mucin.<sup>13</sup> Altered glycosylation in UC can be triggered by disrupted intracellular

glycan synthesis, with over 20 glycoenzymes implicated as UC-associated risk genes.<sup>14</sup> The core 3 synthase, *B3GNT6*, is downregulated in an IBD mouse model, resulting in increased sialyl T and Tn antigens. Conversely, the *ST6GAL1* gene, responsible for the synthesis of  $\alpha$ 2,6-linked sialic acids, contributes to the polarization of CD4+ T cells towards Th<sup>17</sup> cells, thereby activating the IL-17 signaling pathway to promote pro-inflammatory cytokines in UC.<sup>15</sup> Furthermore, UC tissues contain a significantly higher ratio of  $\alpha$ 2,6-linked sialic acid to  $\alpha$ 2,3-linked sialic acids, likely due to the secretion of a neuraminidase (NEU1) with a preference for digesting the latter sialic acid linkage.<sup>16</sup> The decreased abundance of sialic acids disrupts the protective mucus barrier and contributes to inflammation by allowing bacteria to more easily invade the intestinal epithelium.<sup>17</sup> However, the molecular mechanisms underlying these alterations in sialylation in UC remain to be fully elucidated.

This study distinguishes itself from previous investigations of mucosal glycosylation by identifying SIAE as a critical regulator of sialic acid modifications, thereby offering novel insights into the molecular mechanisms driving UC pathogenesis. SIAE plays a crucial role in maintaining normal gut homeostasis by regulating sialic acid acetylation, a process essential for the integrity and function of the mucosal barrier and the fine-tuning of immune responses. By deacetylating sialic acids, SIAE ensures appropriate sialylation patterns that support the protective mucus layer and modulate interactions between immune and epithelial cells, preventing excessive inflammation and maintaining tolerance to commensal bacteria. Therefore, SIAE is critical for proper gut function. While structural analyses of mammalian SIAE have been conducted,<sup>18</sup> the impact of UC-associated mutations on its enzymatic activity and substrate specificity remains largely unexplored. O-acetylation, a common sialic acid modification, is implicated in inflammation. Consequently, SIAE dysfunction may lead to reduced levels of Siglec ligands, potentially lowering the threshold for B cell activation and increasing autoimmune risk.<sup>19</sup> Furthermore, the subtype-specific association of SIAE variants with Juvenile Idiopathic Arthritis phenotypes suggests a role for these variants in adaptive immune dysregulation, particularly in B/T cell interaction abnormalities.<sup>20</sup> Rare and polymorphic SIAE variants, particularly those with functional defects, strongly correlate with susceptibility to common human autoimmune disorders.<sup>21</sup> O-acetyl groups are added to sialic acid through the catalysis of CASD1 and hydrolyzed by SIAE. Studies have shown that UC patients have lower mucin sialic acid O-acetylation compared to normal mucin.<sup>22</sup> However, there is a lack of systematic studies elucidating the molecular mechanisms of SIAE, NEU1, and sialic acids in UC pathogenesis. In this work, we investigated the glycosylation of tissues from UC patients and quantitatively analyzed the expression of key enzymes in tissues and cells. We then investigated the effect of TNF- $\alpha$ -induced inflammation in HT-29 cells to understand how UC can lead to altered cell functions. This research aims to investigate the role of SIAE in UC pathogenesis, with a focus on its influence on sialic acid acetylation, mucosal integrity, and inflammation, employing a combination of proteomic analysis and cell-line experiments.

## Experimental Methods

### Reagents and Materials

Most chemicals and materials were purchased from Beyotime (Shanghai, China), unless otherwise specified. AminoLink™ Plus resin (beads) for protein conjugation was obtained from Thermo Fisher Scientific (Waltham, MA, USA). Sodium citrate ( $\text{Na}_3\text{C}_6\text{H}_5\text{O}_7$ ) and sodium acetate ( $\text{Na}_2\text{CO}_3$ ) were used for the binding buffer. Sodium cyanoborohydride ( $\text{NaCNBH}_3$ ) served as the reducing agent, and 1-hydroxybenzotriazole hydrate (HOBt) was used for ethyl esterification. Polyvinylidene fluoride (PVDF) membranes (0.45  $\mu\text{m}$ ) were used for Western Blotting (WB) (Sigma-Aldrich, St. Louis, MO, USA). N-(3-(Dimethylaminopropyl)-N'-ethylcarbodiimide (EDC) and p-Toluidine (pT) were procured from TCI (Shanghai, China), while formic acid and sodium chloride (NaCl) were obtained from Sinopharm Chemical (Shanghai, China). Glycosidases (PNGase F and  $\alpha$ 2-3,6,8 neuraminidase) were purchased from New England Biolabs (Ipswich, MA, US). Ammonium bicarbonate (ABC), iodoacetamide (IAA), and N,N'-dimethylaniline (DMA) were acquired from Aladdin (Shanghai, China). Tris (2-carboxyethyl) phosphine hydrochloride (TCEP) and trifluoroacetic acid (TFA) were sourced from Macklin (Shanghai, China). High-performance liquid chromatography (HPLC) grade water, acetonitrile (ACN), and 2,5-dihydroxybenzoic acid (DHB) were purchased from J&K Chemical (Zhejiang, China). Sequencing-grade trypsin was obtained from Promega (Madison, WI, USA), and

silica C18 resin was procured from Silicycle (Quebec, QC, Canada). Amide-80 gel slurry (Tosoh Bioscience, Tokyo, Japan) was used as the hydrophilic interaction liquid chromatography stationary absorbent. Empty tubes (1 mL) and frits were utilized to create in-house solid-phase extraction (SPE) cartridges (Biocomma, Shenzhen, China). The HT-29 (CL-0118) cell line was acquired from Pricella (Wuhan, China). SIAE-siRNA was purchased from Genechem (Shanghai, China). HiScript III RT SuperMix for qPCR (+gDNA wiper) and HiScript III RT SuperMix for qPCR (+gDNA wiper) were purchased from VAZYME (Nanjing, China). The PCR primers were ordered from Azenta (Suzhou, China).

## Tissue Sample Preparation

Colon tissue samples from patients with UC, PCA and CA were collected according to a protocol approved by the Ethics Committee of the Second Affiliated Hospital of Soochow University. UC specimens were obtained from UC patients who underwent colonoscopy. Typical lesions in the intestinal cavity were selected for colonoscopy biopsy under direct visualization. After a pathological diagnosis of UC, intestinal segment specimens from these patients were surgically removed, and three samples of active inflammation were selected for inclusion. CA specimens were obtained from patients with colon adenocarcinoma who underwent surgical resection. PCA specimens, confirmed as histologically normal, were obtained from the same CA patients to minimize inter-individual differences. Three samples with a confirmed diagnosis were selected for inclusion. All of the above specimens were obtained with informed consent from the patients, and the experiments were conducted after ethical approval (JD-LI-2021-009-01) in accordance with the Declaration of Helsinki. Colon tissue samples were thoroughly washed with ice-cold 1x PBS to remove blood and other external contaminants, then gently dried using sterile, lint-free tissue. The tissue was weighed using an analytical balance with a precision of 0.1 mg. Subsequently, a volume of pre-chilled RIPA buffer, approximately ten times the tissue weight (~20 mg), was added, along with a 1:100 dilution of 100x protease inhibitors. The tissue was then mechanically lysed using a handheld homogenizer until a uniform mixture was obtained. After homogenization, the lysate was incubated on ice for 20–30 minutes, with gentle vortexing every 5 minutes to enhance protein extraction. Following incubation, the lysate was centrifuged at 12,000 x g for 15 minutes at 4°C. The supernatant, containing the proteins, was carefully transferred into a new tube to avoid disturbing the pellet. The extracted proteins could either be stored on ice for immediate use or frozen at –80°C for long-term preservation.

## Protein Expression by Western Blotting

Proteins were collected from colon tissues and extracted using RIPA lysis buffer for subsequent experiments. The protein solution was mixed with 5x SDS-PAGE loading buffer and heated at 95–100°C for 5 minutes to denature the proteins.<sup>23</sup> 30 µg of denatured protein samples were loaded onto a 10% SDS-PAGE gel. The gel was run using rapid electrophoresis buffer (Beyotime, P0562-10L) at a constant voltage of 150 V for 30 minutes to separate the proteins. Subsequently, an appropriately sized piece of PVDF membrane was cut and placed in transfer buffer (Beyotime, P0575-10L) with an ice pack in the transfer tank. Protein transfer was carried out at a constant current of 400 mA for 30 minutes. The membrane was then incubated in rapid blocking buffer at room temperature for 30 minutes. After blocking, the membrane was incubated with 10 mL of primary antibodies, including SIAE (1:1000 dilution, PA558230, Thermo Fisher Scientific) and GAPDH (1:10000 dilution, 60004-1-Ig, Proteintech), for 1–2 hours at room temperature or overnight at 4°C. The membrane was washed three times with 1x TBST (TBS + 0.1% Tween-20) buffer and subsequently incubated with appropriate horseradish peroxidase (HRP)-conjugated secondary antibodies at room temperature for 1 hour. Two secondary antibodies were used: HRP-labeled goat anti-rabbit IgG (H+L) (1:1000 dilution, A0208) and HRP-labeled goat anti-mouse IgG (H+L) (1:1000 dilution, A0216). Following incubation with secondary antibodies, the membrane was washed three times with 1x TBST buffer. Finally, enhanced chemiluminescence (ECL) reagents (Beyotime, P0018AS) were used for protein detection, and the signals were visualized using a gel imaging system (Chemidoc, Bio-Rad). Each experiment included three technical replicates per sample. The data presented are representative of three independent biological replicates.

## Tissue Immunohistochemistry

Patients with ulcerative colitis (UC) were diagnosed based on standard clinical manifestations, endoscopic examination, and histological criteria (n=10; 5 males, 5 females; age range, 24–45 years). Control intestinal biopsy samples were obtained from paracancerous tissue (PCA) (n = 10; 6 males, 4 females; age range, 45–60 years). Paraffin-embedded tissue sections were deparaffinized by sequential incubation in xylene, graded ethanol solutions (100%, 95%, 80%, 70%), and distilled water (DI). Antigen retrieval was performed by heat-induced epitope retrieval in 10 mM citrate buffer (pH 6.0) at 121°C for 20 minutes. Endogenous peroxidase activity was blocked with 3% hydrogen peroxide for 10 minutes at room temperature. After washing with PBS (pH 7.2), tissues were incubated with a rabbit anti-SIAE antibody (1:200 dilution; Cat. No. PA5-58229; Thermo Fisher) for 2 hours at room temperature. Immunohistochemical staining was performed using a goat anti-rabbit HRP secondary antibody (Cat. No. C31460100) and a metal-enhanced DAB chromogen (Cat. No. 34065). Tissues were counterstained with hematoxylin, dehydrated, and mounted. Stained sections were examined under a microscope and photographed. Consistent with the Western blot (WB) analysis, each experiment included three technical replicates per sample. The data shown are representative of three independent biological replicates.

## N-Glycan Enrichment

Glycoprotein immobilization on Aminolink resin was used to enrich for N-glycans.<sup>24</sup> Approximately 500 µg of protein was dissolved in 100 µL of HPLC water and then added to 200 µL of preconditioned Amino-Link™ Plus resin in 1x PBS within a snap-cap spin-column. The proteins were bound to the resin in 1x binding buffer (5 mM sodium carbonate and 10 mM sodium citrate) for 4 hours at room temperature (RT), followed by incubation with 50 mM NaCNBH<sub>3</sub> for 4 hours to stabilize the binding.<sup>25,26</sup> The resin was subsequently washed three times with 500 µL 1x PBS and further treated with 500 µL 1x PBS containing 50 mM NaCNBH<sub>3</sub> (4 hours up to overnight). The resin was incubated with 1 M Tris-HCl (pH 7.4) (30–60 minutes) to block remaining aldehydes. Sialic acid residues were then derivatized by ethyl esterification (200 µL/0.25 M HOBt and 200 µL/0.25 M EDC in ethanol at 37°C for 1 hour). The resin was washed three times each with 500 µL of ethanol and deionized water (DI), and then further derivatized with a p-toluidine (pT) solution. To prepare the pT solution, 1 M pT was dissolved in 1 N HCl, and the pH was adjusted to 4–6 by adding concentrated HCl (36–38%) to optimize reactivity with sialic acids. The resin was then washed sequentially with 500 µL of 10% formic acid, 10% acetonitrile (ACN), 1 M NaCl, and DI water. 0.5 µL of PNGase F was used to release N-glycans from immobilized glycoproteins in 25 mM ABC, either for 2 hours or overnight at 37°C. The N-glycans solution was then collected by centrifugation, and the resin was washed with 200 µL of 10% ACN to recover any residual N-glycans. Finally, the released N-glycans solution was dried using a Speed-Vac.

## Intact Glycopeptide Preparation

500 µg of proteins was dissolved in 200 µL of 8 M urea in 1 M ABC, then reduced with 25 µL of 120 mM Tris (2-carboxyethyl) phosphine (TCEP) at 37°C for 1 hour. Alkylation was performed by adding 27.5 µL of 160 mM iodoacetamide (IAA) at RT for 1 hour in the dark. The samples were diluted fivefold with HPLC-grade water before digestion with 10 µg sequencing-grade trypsin at 37°C overnight. The reaction was quenched with 10% formic acid (pH < 3), and samples were purified using SPE with a C18 cartridge. Purified peptides were then dissolved in 80% acetonitrile (ACN) with 0.1% trifluoroacetic acid (TFA) for hydrophilic interaction liquid chromatography (HILIC) enrichment. HILIC-SPE column was packed with Amide-80 resin, and samples were loaded twice. The column was washed three times with 80% ACN in 0.1% TFA, then sequentially eluted with solutions containing 60% ACN (0.1% TFA), 40% ACN (0.1% TFA), and 0.1% TFA. The eluate was pooled and evaporated in a Speed-Vac for drying.

## Mass Spectrum Data Analysis

The mass spectrometry data analysis workflow consisted of proteomics and glycoproteomics. For the global analysis, Proteome Discoverer (V2.4.0.305) was used with the “CWF\_Comprehensive\_Enhanced\_Annotation\_LFQ\_and\_Precursor\_Quan” processing workflow and “PWF\_OT\_Precursor\_Quan\_and\_LFQ\_CID\_SequestHT\_Percolator” search engine. The human complete protein database (reviewed) was downloaded from UniProt and used for protein identification. Default settings were used

for variable modifications, including oxidation, dioxidation, deamidation, acetylation, pyro-glutamation of glutamine and glutamic acid, and the fixed modification of carbamidomethylation. In the Sequest HT module, the mass analyzer was set to FTMS, MS2, and HCD. Byonic (version 4.3.4) was used for the analysis of mass spectrometry data from HILIC enriched glycopeptides. The enzyme specificity was set to trypsin with cleavage at Lysine (K) and arginine (R) residues, allowing for a maximum of two missed cleavages. Mass tolerances were set at 10 ppm for precursor ions and 20 ppm for fragment ions. A q-value threshold of 0.05 was used. Carbamidomethylation was set as a fixed modification, and variable modifications included oxidation, deamidation, dethiomethylation, and pyro-glutamation of glutamine and glutamic acid. A multi-part g-Gaussian mixture model was used to estimate the false discovery rate (FDR), with a 1% PSM FDR threshold. Finally, LC-MS/MS data were analyzed by matching MS2 spectra to a glycopeptide spectral library built from a human glycoprotein FASTA file downloaded from Uniprot. The glycan database used was mammalian N-glycan with sialic acids modified by acetyl. Protein-protein interaction analysis was performed using GeneMANIA.<sup>27</sup> Due to limited tissue availability, technical replicates were not performed for the MS analysis. However, the results were validated across three biological replicates.

## Confocal Microscope on Cell Surface Sialic Acid Expression

HT-29 cells were treated with DMSO (negative control), TNF- $\alpha$  (100 ng/mL for 24 hours), or  $\alpha$ 2-3,6,8 neuraminidase (NEU) (500 U/mL for 1 hour) (positive control), respectively, at 37°C in a humidified atmosphere containing 5% CO<sub>2</sub>. Cells were cultured in 500 U/mL NEU for 1 hour at 37°C in a humidified 5% CO<sub>2</sub> incubator without serum. Subsequently, cells were fixed with 4% paraformaldehyde for 10 minutes at room temperature. Cell surface sialic acid content was stained with FITC-conjugated Sambucus nigra lectin (SNA) diluted 1:400 in PBS for 1 hour at room temperature. DAPI was used to stain the nuclei. Cells were visualized using a Nikon AX confocal microscope.

## Results and Discussion

### Sialic Acid Acetylation Present on UC Tissue

To detect sialic acid acetylation, we extracted proteins from UC and PCA tissues for glycan analysis. Given the fragility of sialic acids, which are easily lost at lower pH or during matrix-assisted laser desorption ionization (MALDI), we stabilized sialic acids through one- or two-step chemical derivatization.<sup>25,26,28</sup> Studies have shown that acetyl esters can modify N-acetylneuraminic acid (Neu5Ac) at the 4-, 7-, and 9-positions, resulting in up to 15 different O-acetylation patterns.<sup>19,29</sup> Because the carboxylic acid at the 1-position remains unaffected by acetylation, chemical derivatization of the carboxylic acid preserves acetylated Neu5Ac stability. To enrich N-glycans, we extracted proteins from colon tissues with ulcerative colitis (UC) and paracancerous (PCA) and conjugated them with aldehyde-functionalized resin (AminoLink Plus, Thermo). Sequential ethanol esterification and p-toluidine reductive amination derivatized the carboxylic acid of Neu5Ac, converting  $\alpha$ 2,6-linked and  $\alpha$ 2,3-linked sialic acids into stable esters and amides, respectively.<sup>26</sup> This enabled MALDI-TOF-MS analysis without loss of fragile sialic acids. Our results indicated that the most abundant N-glycans in both UC and PCA were high-mannose, with sialoglycans present in both UC and PCA (Figure 1). Importantly, we detected acetylated sialic acids from MALDI analysis, such as the mass (m/z) at 2171.1 Da, suggesting that acetylation occurs in UC and warrants further investigation.

### Dysregulated N-Glycan Expression in UC and CA Tissues

We further investigated the distribution of N-glycan subsets in UC, colon cancer (CA), and PCA. N-glycans were categorized as high-mannose (Figure 2A), fucosylated N-glycans (Figure 2B), sialoglycans (Figure 2C), and N-glycans without fucose or sialic acid (Figure 2D). High-mannose N-glycans were generally more abundant in UC compared to CA or PCA, with Man5 (H5N2) showing a statistically significant difference among these groups, decreasing from UC to CA to PCA. Fucosylated N-glycans exhibited a different profile, with CA showing higher abundance of fucosylation, particularly on H3N4F1 and H4N4F1 (Figure 2B). Conversely, sialic acids were most abundant in PCA and less abundant in UC and CA (Figure 2C). Additionally, galactosylated N-glycans were slightly higher in PCA. The potential mechanisms underlying these variations will be explored in this study.

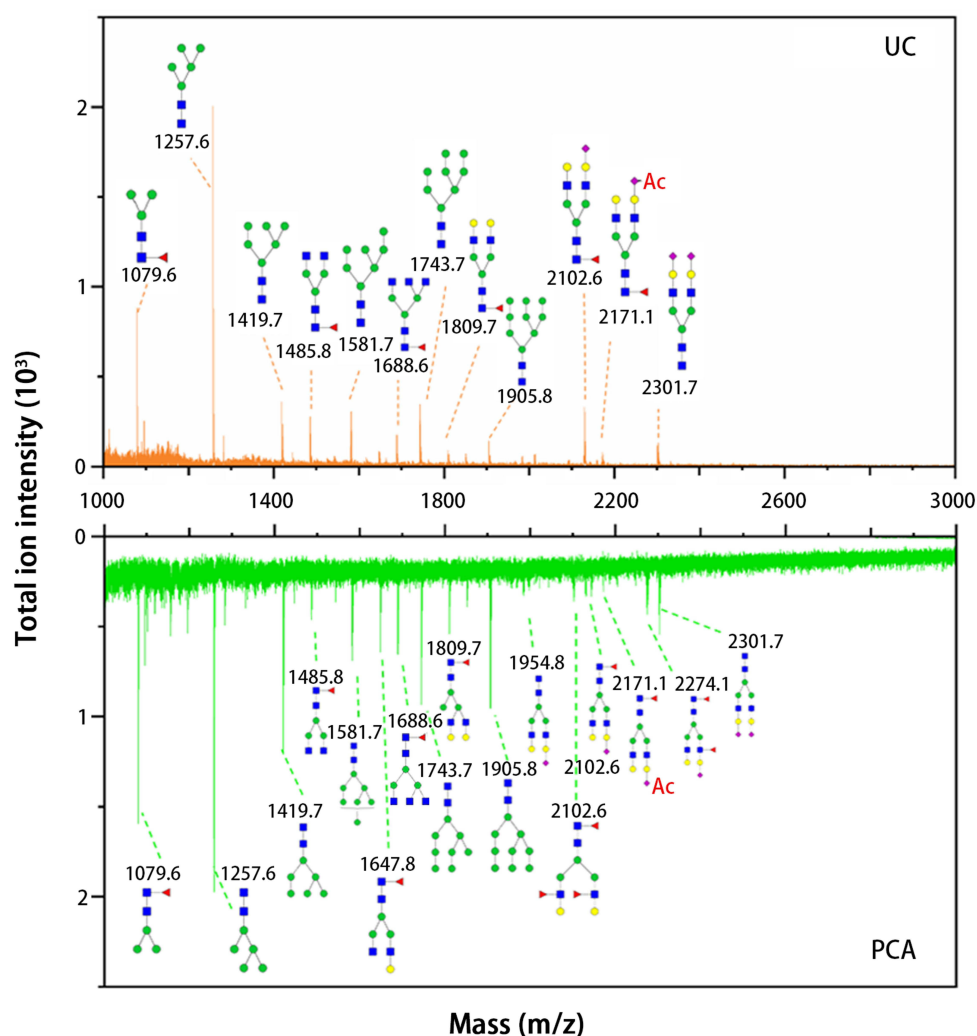


**Figure 1** MALDI-TOF-MS comparison of glycan profiles in ulcerative colitis (UC) and paracancerous (PCA) tissues. Acetylated sialic acids are detected in both UC and PCA. Technical replicates were performed in triplicate, with a standard deviation of less than 10%.

## Contributes to Colonic Inflammation and Tumor Development

While alterations in sialic glycosylation patterns in UC have been reported,<sup>30</sup> our study establishes that SIAE directly links enzyme deacetylation activity to disease-specific sialylation characteristics. To understand the potential mechanisms underlying decreased sialylation in UC and CA, and to investigate whether acetylation is reduced in disease, we first analyzed the global proteome of these tissues. Tryptic peptides were analyzed by nano-LC-MS/MS, while MS spectra were analyzed using Proteome Discoverer (V2.4.0.305). The Venn diagram in [Figure 3A](#) shows that over 2000 proteins are concurrently present in UC, CA, and PCA. Volcano plots reveal dysregulated proteins in both UC and CA, although the specific dysregulated proteins differ between the two conditions. These altered proteins were selected for KEGG pathway analysis based on their genes in combination with ShinyGO 0.81 bioinformatics.<sup>31</sup> The identified pathways have been generally correlated to the development and progression of UC.

[Table 1](#) summarizes primary signaling pathways involved in UC pathogenesis. Among them, the complement and coagulation cascades (CCC) may contribute to UC development and progression by promoting inflammation through mutual activation and the release of inflammatory mediators like cytokines or chemokines.<sup>32,33</sup> Activated platelets release pro-inflammatory mediators such as IL-1, soluble P-selectin, or CD40 ligand, thereby exacerbating mucosal damage,<sup>34,35</sup> while neutrophil extracellular traps (NETs) release DNA-based structures, damaging the mucosa and worsening the disease.<sup>36</sup> Notably, activation of the nicotinate and nicotinamide metabolism pathway may induce severe inflammation by

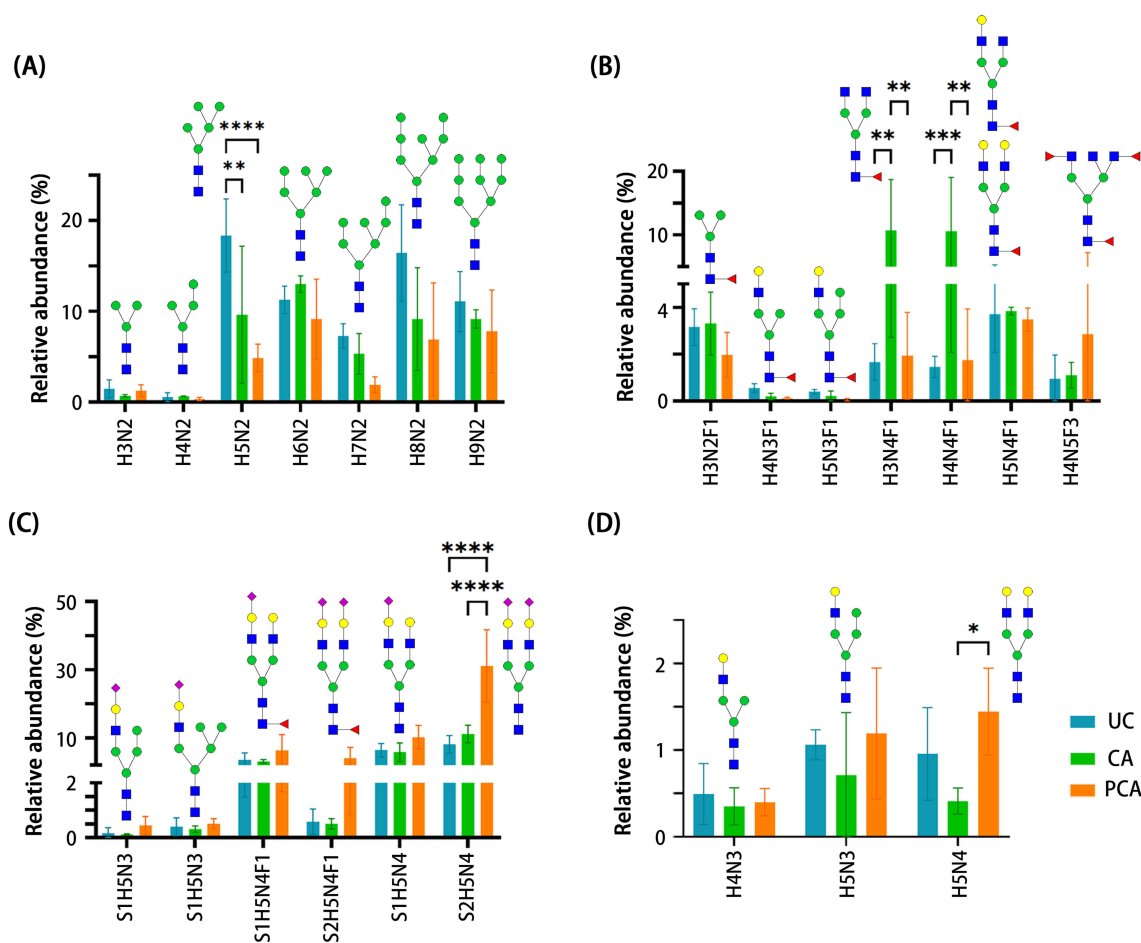


**Figure 2** LC-MS/MS comparison of glycan profiles in ulcerative colitis (UC), colon cancer (CA), and paracancerous (PCA) tissues. **(A)** High-mannose N-glycans, such as H3N2, H4N2, and H5N2, are significantly more abundant in UC compared to CA and PCA. **(B)** Fucosylated N-glycans, including H3N2F1, H4N2F1, and H5N2F1, are enriched in CA. **(C)** Sialic acid-containing glycans, particularly S1H5N3 and S2H5N4, are slightly elevated in PCA. **(D)** Galactosylated N-glycans, like H3N3 and H5N3, show a slight increase in abundance in PCA. H = Hexose, N = HexNAc, F = Fucose, S = Neu5Ac. Data analyzed ANOVA analysis (\*p < 0.05, \*\*p < 0.01, \*\*\*p < 0.001, \*\*\*\*p < 0.0001).

cell-cell interactions in UC, with inflamed tissues exhibiting decreased NAD<sup>+</sup> levels and increased nicotinamide (NAM) levels.<sup>37,38</sup> The renin-angiotensin system (RAS) promotes colonic inflammation by stimulating TH<sup>17</sup> activation, and RAS inhibitors have been effective in preclinical studies.<sup>39</sup> Interestingly, pancreatic disorders are associated with UC, with a higher incidence in UC and CD patients.<sup>40</sup> Other pathways related to UC are also summarized in Table 1.<sup>41–44</sup> Meanwhile, the potential biological roles of proteins up- or down-regulated in colon cancer, as shown in the volcano plot (Figure 3A), are illustrated in Table S2. These proteins are widely implicated in tumor development and progression.

Immunohistochemistry (IHC) revealed increased expression of SIAE in both UC and CA tissues. Western blot (WB) analysis also confirmed higher SIAE expression in UC and CA compared to PCA (Figure 3B and C). WB analysis demonstrated that SIAE protein concentration was lowest in PCA, intermediate in UC, and highest in CA. This finding aligns with the TCGA dataset, which showed significantly higher SIAE expression in colon adenocarcinomas (COAD) (Figure S1). The SIAE gene expression in tumor tissue was 2.66-fold higher than in normal tissue, although there was negligible difference in expression from stage 1 to 4. Quantitative WB analysis of tissue specimens revealed over 2-fold higher protein expression in UC, suggesting a substantial increase in SIAE in UC. GeneMANIA analysis indicated that SIAE correlates with numerous glycoproteins (Figure 3D), hinting at its potential involvement in the de-acetylation of these glycoproteins.

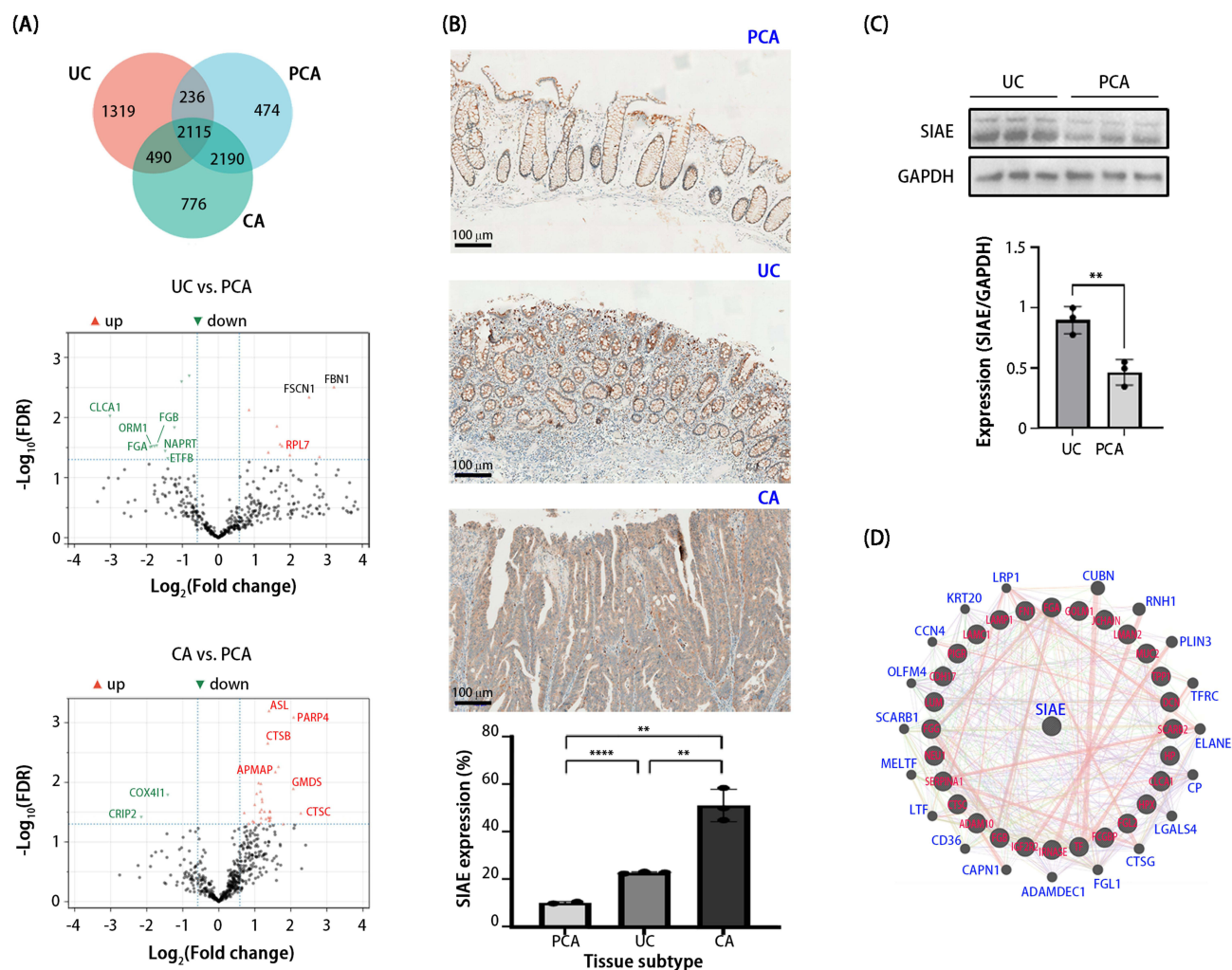


**Figure 3** Deacetylation of sialic acids in ulcerative colitis (UC) and precancerous tissue promotes inflammation and may contribute to carcinogenesis. **(A)** Global proteomic analysis revealed significant alterations in protein expression in UC and colon cancer (CA) tissues, including upregulation of proteins involved in inflammatory pathways. Volcano plot of differentially abundant proteins (Welch's *t*-test,  $\log_2FC > 1$ , FDR-adjusted  $q < 0.05$ ) **(B and C)** Immunohistochemistry (IHC) and Western blot analyses demonstrated increased expression of sialic acid acetyltransferase (SIAE) in UC and CA tissues. Data analyzed by unpaired two-tailed *t*-test (\*\* $p < 0.01$ , \*\*\*\* $p < 0.001$ ) **(D)** Protein-protein interaction studies indicated that SIAE interacts with glycoproteins, such as MUC2, suggesting a potential role in modulating mucus layer integrity and inflammation.

## Site-Specific Sialic Acid Acetylation in Glycoproteins

Previous studies have demonstrated that the concentration of O-acetylated sialic acids in the gastrointestinal tract diminishes in diseases such as colorectal adenocarcinoma,<sup>45,46</sup> myeloma,<sup>47</sup> and UC.<sup>48</sup> LC-MS/MS analysis revealed distinct patterns of sialic acid acetylation within identified glycoproteins (Table 2). Sialic acids containing acetylation were identified in tissues from patients with PCA, UC, and CA, each exhibiting unique glycoproteins with acetylated sialic acids (Table S3). Acetylated glycoproteins potentially involved in mucosal protection include cadherin-17 (*CDH17*), mucin 2 (*MUC2*), calcium-activated chloride channel regulator 1 (*CLCA1*), scavenger receptor class B member 2 (*SCARB2*), Fc gamma binding protein (FCGBP), polymeric immunoglobulin receptor (*PIGR*), haptoglobin (*HP*), lumican (*LUM*), transferrin (*TF*), hemopexin (*HPX*), and decorin (*DCN*). Fourteen glycoproteins were co-expressed in tissues from patients with UC and PCA, thirteen of which were also detected in CA (Figure 4A).

Figure 4B highlights two heavily acetylated examples, showcasing their N-glycosylation sites and associated modifications. Notably, *CDH17*, a crucial protein for intestinal cell adhesion (also known as liver-intestine cadherin), possesses four N-glycosylation sites (N250, N419, N587, N722). Interestingly, the types of acetylated N-glycans vary among patient groups (PCA, UC, CA), with PCA exhibiting diverse sialic acid acetylation. *CDH17*, an intestinal

**Table 1** The Genes Involved in the Signaling Pathways of Ulcerative Colitis

| Pathway                                 | Enrichment FDR | Fold Enrichment | Gene                       | Role in UC  |
|---|----------------|-----------------|----------------------------|---|
| Complement and coagulation cascades     | 4.04E-03       | 48.9            | <i>FGA</i> ,<br><i>FGB</i> | Activation of complement and coagulation cascades contributes to the development and progression of UC, as well as tissue damage within the gut lining. <sup>32</sup>   |
| Platelet activation                     | 5.69E-03       | 33.5            | <i>FGA</i> ,<br><i>FGB</i> | Platelet activation contributes to UC within the colon by releasing pro-inflammatory mediators, thereby amplifying the inflammatory response and contributing to mucosal damage. <sup>34</sup>  |
| Neutrophil extracellular trap formation | 9.77E-03       | 22.0            | <i>FGA</i> ,<br><i>FGB</i> | Neutrophil extracellular trap (NET) formation occurs when neutrophils are activated by inflammatory stimuli in UC, resulting in the release of DNA-based structures containing granule proteins. These structures can damage the intestinal mucosa and contribute to disease progression. <sup>36</sup> |
| Nicotinate and nicotinamide metabolism  | 3.78E-02       | 57.8            | <i>NAPRT</i>               | Nicotinate and nicotinamide metabolism is implicated in UC. Inflamed UC tissues demonstrate decreased NAD <sup>+</sup> levels and increased levels of its breakdown products, such as nicotinamide (NAM). <sup>37</sup>   |
| Renin secretion                         | 5.99E-02       | 30.1            | <i>CLCA1</i>               | Renin-angiotensin system promotes UC by partially stimulating TH <sup>17</sup> activation. <sup>39</sup>  |
| Pancreatic secretion                    | 6.60E-02       | 20.4            | <i>CLCA1</i>               | Pancreatic disorders are commonly observed in individuals with UC. <sup>40</sup>  |
| Staphylococcus aureus infection         | 6.60E-02       | 22.1            | <i>KRT20</i>               | When <i>Staphylococcus aureus</i> enters the gut mucosa, it triggers an UC response by activating immune cells through the recognition of bacterial components, such as lipopolysaccharides. This activation leads to further tissue damage and potentially exacerbates colitis symptoms. <sup>41</sup> |
| Ribosome                                | 7.08E-02       | 15.5            | <i>RPL7</i>                | A dysregulation in the ribosome pathway is significantly linked to the development of UC <sup>42,43</sup>   |
| Estrogen signaling                      | 7.08E-02       | 15.1            | <i>KRT20</i>               | Estrogen receptor beta (ERβ) plays a protective role by maintaining intestinal epithelial cell homeostasis and inhibiting UC within the colon <sup>44</sup>   |

**Abbreviations:** FGA, Fibrinogen alpha chain; FGB, Fibrinogen beta chain; NAPRT, Nicotinate phosphoribosyltransferase; CLCA1, Calcium-activated chloride channel regulator 1; KRT20, Type I cytoskeletal 20 keratin; RPL7, Large ribosomal subunit protein uL30.

**Table 2** Altered Glycoproteins in Tissues From Patients With Ulcerative Colitis (UC) and Colon Cancer (CA)

| Accession | Gene           | UC/PCA |       | CA/PCA |       |
|-----------|----------------|--------|-------|--------|-------|
|           |                | FC     | SD    | FC     | SD    |
| P00450    | <i>CP</i>      | 0.899  | 0.031 | 0.782  | 0.145 |
| P11117    | <i>ACP2</i>    | 2.026  | 0.088 | 1.735  | 0.084 |
| P26006    | <i>ITGA3</i>   | 0.914  | 0.171 | 0.477  | 0.111 |
| P10619    | <i>CTSA</i>    | 1.087  | 0.534 | 0.488  | 0.372 |
| Q92542    | <i>NCSTN</i>   | 0.406  | 0.116 | 0.702  | 0.044 |
| Q9Y5Y6    | <i>ST14</i>    | 1.482  | 0.097 | 1.614  | 0.16  |
| P56199    | <i>ITGA1</i>   | 0.66   | 0.205 | 0.642  | 0.748 |
| P11047    | <i>LAMC1</i>   | 0.888  | 0.198 | 0.399  | 0.248 |
| P10253    | <i>GAA</i>     | 0.81   | 0.115 | 1.244  | 0.316 |
| O95302    | <i>FKBP9</i>   | 0.896  | 0.08  | 1.456  | 0.396 |
| P07711    | <i>CTSL</i>    | 1.228  | 0.283 | 1.09   | 0.415 |
| P13688    | <i>CEACAM1</i> | 10.516 | 0.846 | 2.581  | 0.17  |
| P51884    | <i>LUM</i>     | 0.095  | 0.404 | 0.103  | 9.449 |
| Q8TCJ2    | <i>STT3B</i>   | 2.481  | 0.564 | 1.298  | 0.835 |
| P0DOX6    | <i>/</i>       | 1.67   | 0.285 | 2.186  | 0.14  |
| O14672    | <i>ADAM10</i>  | 0.594  | 0.264 | 1.525  | 0.938 |

(Continued)

Table 2 (Continued).

| Accession     | Gene            | UC/PCA       |              | CA/PCA        |              |
|---------------|-----------------|--------------|--------------|---------------|--------------|
|               |                 | FC           | SD           | FC            | SD           |
| P50897        | <i>PPT1</i>     | 2.638        | 0.089        | 5.67          | 0.197        |
| Q9Y4LI        | <i>HYOU1</i>    | 2.525        | 1.158        | 2.378         | 1.199        |
| Q9HDC9        | <i>APMAP</i>    | 1.754        | 0.428        | 2.121         | 0.603        |
| P01024        | <i>C3</i>       | 0.587        | 0.997        | 0.587         | 1.829        |
| P46977        | <i>STT3A</i>    | 2.239        | 1.555        | 1.053         | 1.285        |
| P02675        | <i>FGB</i>      | 0.462        | 0.941        | 0.779         | 3.141        |
| Q08380        | <i>LGALS3BP</i> | 0.688        | 0.092        | 3.189         | 0.117        |
| P07686        | <i>HEXB</i>     | 0.198        | 0.092        | 1.734         | 0.593        |
| O14773        | <i>TPPI</i>     | 0.779        | 0.336        | 0.968         | 1.331        |
| P23229        | <i>ITGA6</i>    | 0.636        | 0.117        | 2.264         | 0.339        |
| P02787        | <i>TF</i>       | 0.479        | 0.531        | 0.453         | 4.146        |
| P53634        | <i>CTSC</i>     | 18.72        | 1.061        | 8.94          | 0.176        |
| P08236        | <i>GUSB</i>     | 0.613        | 0.039        | 3.208         | 0.277        |
| P01009        | <i>SERPINA1</i> | 0.809        | 1.848        | 1.275         | 0.658        |
| Q13510        | <i>ASAH1</i>    | 1.506        | 0.503        | 2.88          | 0.43         |
| P07585        | <i>DCN</i>      | 0.376        | 1.407        | 0.247         | 6.953        |
| Q9Y6R7        | <i>FCGBP</i>    | 0.448        | 0.816        | 1.886         | 1.417        |
| A8K7I4        | <i>CLCA1</i>    | 0.99         | 3.225        | 1.213         | 5.526        |
| P02790        | <i>HPX</i>      | 0.116        | 0.56         | 0.216         | 11.772       |
| P43308        | <i>SSR2</i>     | 6.906        | 7.416        | 2.387         | 3.01         |
| P01591        | <i>JCHAIN</i>   | 1.626        | 2.838        | 1.194         | 2.686        |
| Q02817        | <i>MUC2</i>     | 2.983        | 6.05         | 3.415         | 2.785        |
| P02679        | <i>FGG</i>      | 1.09         | 1.121        | 3.88          | 0.382        |
| P14625        | <i>HSP90B1</i>  | 4.41         | 3.878        | 3.023         | 3.336        |
| P10153        | <i>RNASE2</i>   | 1.559        | 6.686        | 0.782         | 4.841        |
| P00738        | <i>HP</i>       | 0.516        | 1.415        | 1.449         | 3.601        |
| <b>Q9HAT2</b> | <b>SIAE</b>     | <b>4.942</b> | <b>0.071</b> | <b>10.252</b> | <b>0.006</b> |

**Notes:** Fold change values are calculated relative to paracancerous tissue (PCA). Protein accession numbers are obtained from the UniProt human protein database. Differential proteins (FC > 1, SD < 0.05) are shown in bold.

**Abbreviations:** FC, Fold change; SD, Standard deviation.

epithelial adhesion molecule whose deletion has been found to enhance intestinal permeability in a mouse model,<sup>49</sup> may be further compromised by SIAE-mediated hydrolysis of sialic acid acetylation, potentially increasing epithelial permeability. Similarly, the sialylation of *MUC2*, the major component of the mucosal layer,<sup>50</sup> contributes to its negative charge, facilitating the formation of the mucosal layer to combat bacterial invasion. Loss of acetylation and sialylation can weaken epithelial cell defense against bacterial or chemical invasion. While HLA-A (an immune antigen) exhibits highly branched N-glycans with acetylated sialic acids in UC patients, SIAE itself (an N-glycoprotein) lacks this modification across all groups, despite slight variations in their glycan profiles. These findings suggest that SIAE-mediated sialic acid de-acetylation plays a significant role in UC pathogenesis and may serve as a potential biomarker or therapeutic target.<sup>51</sup>

## SIAE-Induced Reduction of Sialic Acid and Acetylation in UC

To induce inflammation, we treated the HT-29 cell line with varying concentrations of TNF- $\alpha$ .<sup>52</sup> It is reported in the literature that dose concentrations in the range of 10–100 ng/mL are typically employed in inflammatory modeling.<sup>53</sup> Real-time qPCR (RT-qPCR) analysis revealed that SIAE expression increased with an elevated TNF- $\alpha$  concentration up to 100 ng/mL, suggesting that TNF- $\alpha$  triggered inflammation in HT-29 cells and led to decreased sialic acid acetylation (Figure 5A). We selected a TNF- $\alpha$  concentration of 100 ng/mL for subsequent experiments, as it exhibited the highest

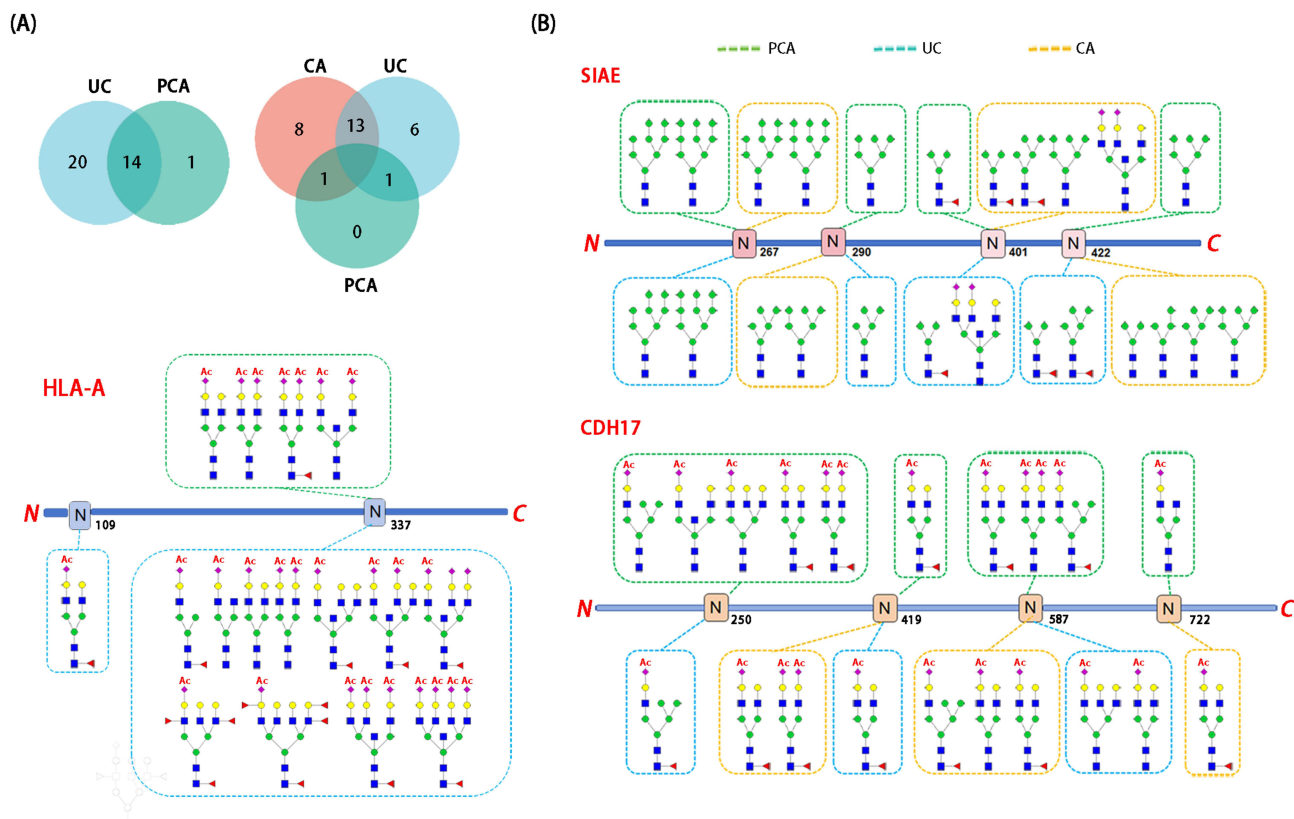


**Figure 4** Site-specific identification of acetylated sialoglycoproteins by LC-MS/MS. **(A)** Venn diagram illustrating the overlap of identified glycoproteins carrying sialic acid acetylation among ulcerative colitis (UC), Colon cancer (CA), and paraneoplastic (PCA) samples. **(B)** Structural representations of three sialoglycoproteins (SIAE, CDH17, and HLA-A) identified in UC, CA, and PCA. While SIAE possesses four potential N-glycosylation sites, mass spectrometry analysis indicated that the sialic acids attached to these sites are not acetylated. In contrast, CDH17 and HLA-A proteins exhibit numerous acetylated sialic acids. Green dot line = Glycans from PCA, Blue dot line = Glycans from UC, Yellow dot line = Glycans from CA.

expression at this concentration. Next, we collected TNF- $\alpha$ -treated cells and performed RT-PCR to determine whether cell-cell adhesion was affected by inflammation. RT-PCR showed that E-cadherin (*CDH1*) was decreased after TNF- $\alpha$  treatment, concurrently reducing the expression of catenin delta 1 (*CTNND1*) (Figure 5B). Both of these proteins are closely correlated with carcinoma invasiveness.<sup>54</sup> Other cell-cell adhesion genes were also downregulated, such as integrins (*ITGA8*) and collagens (*COL6A2*, *COL1A1*). These results suggest that cell-cell adhesion is attenuated by inflammatory responses, leading to increased mucosal barrier permeability.<sup>55</sup>

We then studied whether cell-cell adhesion relates to altered sialylation. HT-29 cells were treated with 100 ng/mL of TNF- $\alpha$  for 24 hours. A negative control and a positive control were prepared by adding DMSO and  $\alpha$ 2-3,6,8 neuraminidase (NEU), respectively. To detect  $\alpha$ 2-6 linked sialic acid (a major form in HT-29 cells), we used Sambucus Nigra Lectin (SNA) labeled with AF488 fluorescein. Western blot (WB) showed that SIAE expression was upregulated in TNF- $\alpha$ -treated HT-29 cells (Figure 5C). NEU-treated cells should have less sialylation as NEU hydrolyzes  $\alpha$ 2-3,6,8 linked sialic acids, while control (DMSO) cells have the highest sialylation. However, TNF- $\alpha$ -treated cells should have sialylation between DMSO and NEU-treated cell lines. Figure 5C showed that TNF- $\alpha$ -treated cells indeed have lower sialylation compared to DMSO-treated cells but higher than NEU-treated cells. Confocal microscopy revealed that sialic acids are located on the cellular surface, as SNA lectin specifically binds  $\alpha$ 2,6 linked sialic acids. The higher expression of SIAE in TNF- $\alpha$ -treated cells, quantified by WB, suggests that SIAE upregulation ultimately leads to the degradation of sialic acids. Notably, NEU-treated cells show the presence of  $\alpha$ 2,6-linked sialic acids. This may be due to sialylation on RNA that cannot be completely digested by neuraminidase, as RNA sialylation has been found on the cell surface.<sup>56,57</sup> A reduction in sialic acid levels is observed in UC, particularly on the surface of intestinal mucosal cells. This decrease in sialic acid is considered a key factor contributing to the inflammation and damage seen in

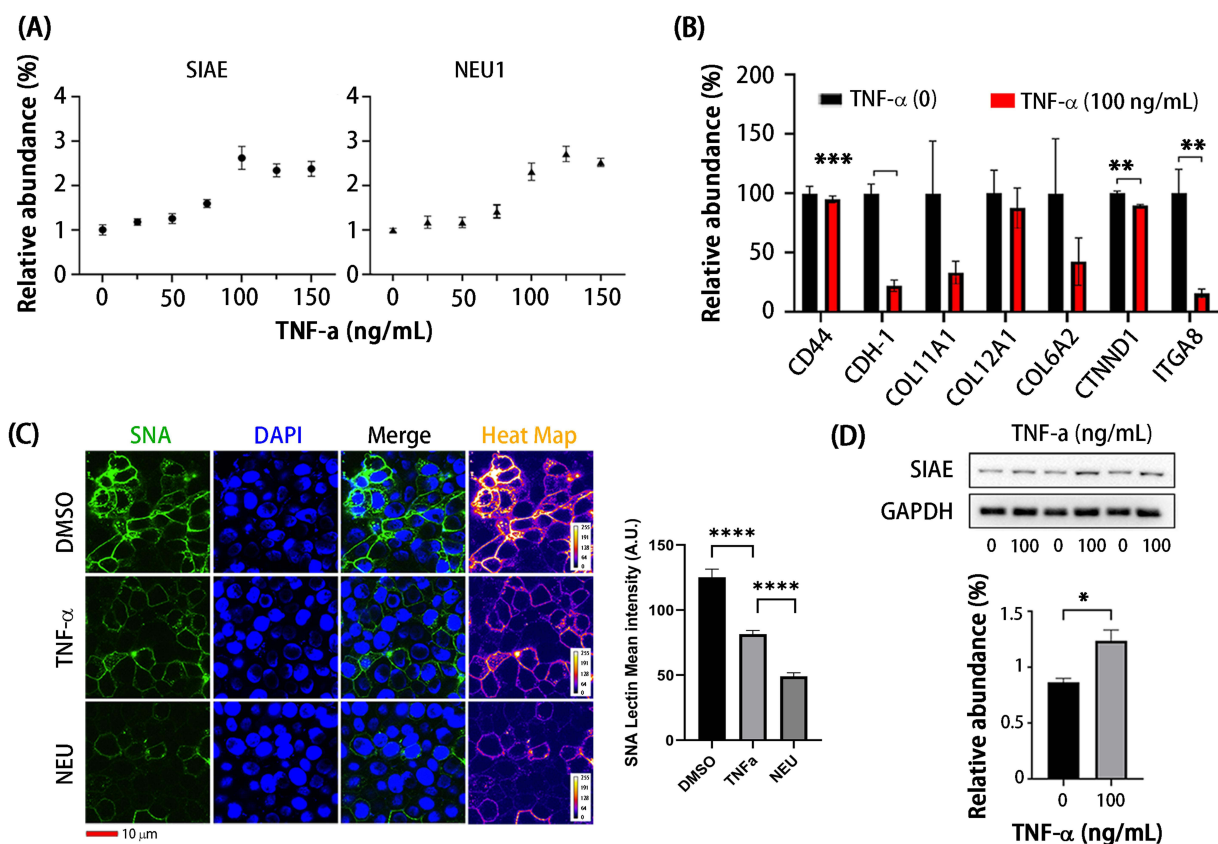


**Figure 5** Upregulated SIAE in TNF- $\alpha$ -induced ulcerative colitis and reduced cellular surface sialylation. **(A)** RT-qPCR quantification of SIAE and NEU1 expression in HT-29 cells treated with increasing concentrations of TNF- $\alpha$ . **(B)** Gene expression analysis of cellular proteins in HT-29 cells treated with 100 ng/mL TNF- $\alpha$ . Cellular surface proteins *CDH-1*, *CTNND1*, and *ITGA8* are downregulated under inflammatory conditions. Western blot (WB) analysis confirms the upregulation of SIAE in HT-29 cells treated with 100 ng/mL TNF- $\alpha$ . **(C)** Fluorescein-labeled SNA lectin staining reveals reduced sialic acid expression on the cell surface of TNF- $\alpha$ -treated HT-29 cells (100 ng/mL).  $\alpha$ 2-3,6,8 Neuraminidase (NEU)-treated cells serve as a positive control. Data analyzed by unpaired two-tailed t-test (\*p < 0.05, \*\*p < 0.01, \*\*\*p < 0.001, \*\*\*\*p < 0.0001).

UC through neutrophil transepithelial migration and CD11b/CD18 activation.<sup>58</sup> The reduced sialic acid levels can potentially lead to increased bacterial adhesion and immune response activation within the gut lumen.<sup>16</sup> These results revealed that UC pathogenesis may involve the SIAE-participated signaling pathway. Unlike previous studies, the specificity of this mechanism positions SIAE as a potential drug target, offering a more focused approach than broad glycosylation pathway interventions.

## Limitations of the Study

The small sample size (three biological replicates per group, each with three technical replicates) may affect statistical significance. To further validate our findings, future work should include larger sample sizes and more in-depth functional studies, such as investigating the effects of prolonged TNF- $\alpha$  stimulation. Also, we did not perform a stratified analysis of patient data based on gender, age, or other relevant factors.

## Conclusion

Ulcerative colitis (UC) is a chronic disease with no effective treatment. Understanding its pathogenesis is crucial for early diagnosis and drug target identification. In this study, we investigated the changes in proteins and glycoproteins in UC compared to healthy controls. We found that sialic acids and their acetylation are reduced in tissues of patients with UC, while sialylation and O-acetylation are more abundant in healthy controls. Mass spectrometry analysis revealed that SIAE, an enzyme that hydrolyzes sialic acid acetylation, is upregulated in UC. Sialic acid, particularly when acetylated, plays a protective role in the colon by preventing inflammation through mechanisms such as modulating immune cell

interactions and shielding the intestinal lining from harmful bacteria, acting as a barrier against excessive immune response in the gut.<sup>45</sup> The colonic inflammation induced by TNF- $\alpha$  drives the upregulation of SIAE and NEU1, leading to deacetylation and desialylation. Further experiments using HT-29 cells exposed to TNF- $\alpha$  confirmed these findings. We observed a 5-fold increase in SIAE and NEU1 expression, a reduction in sialic acid acetylation and overall sialic acid levels, and a decrease in cell-cell adhesion markers. These results suggest that SIAE contributes to UC progression by compromising mucosal protection through the hydrolysis of sialic acid acetylation and reduction of sialic acids.

In summary, this study demonstrates that sialic acid acetyltransferase (SIAE) plays a crucial role in UC pathogenesis by modulating sialic acid acetylation and subsequently disrupting mucosal integrity. This finding advances our understanding beyond previous studies focused solely on general glycosylation alterations in UC, by specifically identifying SIAE as a key regulatory enzyme. Unlike broad glycosylation pathway interventions, the specificity of SIAE suggests that it represents a potentially druggable node, offering a more targeted therapeutic approach. Our results indicate that small molecule inhibitors targeting SIAE could emerge as a novel therapeutic strategy for UC, potentially leading to improved disease management. However, we acknowledge limitations, including the small sample size and the focus on acute TNF- $\alpha$  stimulation, which may limit the generalizability of our findings. Future studies with larger patient cohorts and investigations of long-term inflammatory effects are warranted to validate these results and further explore the therapeutic potential of SIAE inhibition in UC.

## Acknowledgments

This research has received financial support from the Soochow University Start-up Fund. We extend our gratitude to the Priority Academic Program Development of the Jiangsu Higher Education Institutes (PAPD), the Jiangsu Science and Technology Plan Funding (BX2022023), the Jiangsu Shuangchuang Boshi Funding (JSSCBS20210697), the Suzhou Health Youth Talent Project (GSWS2022087), the Suzhou Science and Technology Plan Funding (SYW2024037), the Project of State Key Laboratory of Radiation Medicine and Protection (GZK12023012), the Science and Technology Development Program Project of Suzhou (SKYD2022032, SKY2023055), the Pilot Project of the National Natural Science Foundation of China (SDFEYGJ2021), and the Open Project of Jiangsu Provincial Key Laboratory of Medical Optics (JKLMO 202202).

## Author Contributions

All authors made a significant contribution to the work reported, whether that is in the conception, study design, execution, acquisition of data, analysis and interpretation, or in all these areas; took part in drafting, revising or critically reviewing the article; gave final approval of the version to be published; have agreed on the journal to which the article has been submitted; and agree to be accountable for all aspects of the work.

## Disclosure

The authors declare no competing financial interests.

## References

1. Lewis JD, Parlett LE, Jonsson Funk ML, et al. Incidence, prevalence, and racial and ethnic distribution of inflammatory bowel disease in the United States. *Gastroenterology*. 2023;165:1197–1205.e2. doi:10.1053/j.gastro.2023.07.003
2. Alatab S, Sepanlou SG, Ikuta K, et al. The global, regional, and national burden of inflammatory bowel disease in 195 countries and territories, 1990–2017: a systematic analysis for the global burden of disease study 2017. *Lancet Gastroenterol Hepatol*. 2020;5:17–30. doi:10.1016/S2468-1253(19)30333-4
3. Orholm M, Munkholm P, Langholz E, Nielsen Ole H, Sørensen Thorkild IA, Binder V. Familial occurrence of inflammatory bowel disease. *N Engl J Med*. 1991;324:84–88. doi:10.1056/NEJM199101103240203
4. Cho JH, Brant SR. Recent insights into the genetics of inflammatory bowel disease. *Gastroenterology*. 2011;140:1704–1712.e2. doi:10.1053/j.gastro.2011.02.046
5. Pereira GV, Boudaud M, Wolter M, et al. Opposing diet, microbiome, and metabolite mechanisms regulate inflammatory bowel disease in a genetically susceptible host. *Cell Host Microbe*. 2024;32:527–542.e9. doi:10.1016/j.chom.2024.03.001
6. Molodecky NA, Kaplan GG. Environmental risk factors for inflammatory bowel disease. *Gastroenterol Hepatol*. 2010;6:339–346.
7. Le Berre C, Honap S, Peyrin-Biroulet L. Ulcerative colitis. *Lancet*. 2023;402:571–584. doi:10.1016/S0140-6736(23)00966-2
8. Gajendran M, Loganathan P, Jimenez G, et al. A comprehensive review and update on ulcerative colitis. *Dis Mon*. 2019;65:1–37.

9. Alipour M, Zaidi D, Valcheva R, et al. Mucosal barrier depletion and loss of bacterial diversity are primary abnormalities in paediatric ulcerative colitis. *J Crohns Colitis*. 2016;10:462–471. doi:10.1093/ecco-jcc/jjv223
10. Johansson MEV, Larsson JMH, Hansson GC. The two mucus layers of colon are organized by the MUC2 mucin, whereas the outer layer is a legislator of host–microbial interactions. *Proc Natl Acad Sci USA*. 2011;108:4659–4665. doi:10.1073/pnas.1006451107
11. Schroeder BO. Fight them or feed them: how the intestinal mucus layer manages the gut microbiota. *Gastroenterol Rep*. 2019;7:3–12. doi:10.1093/gastro/goy052
12. Kudelka MR, Stowell SR, Cummings RD, Neish AS. Intestinal epithelial glycosylation in homeostasis and gut microbiota interactions in IBD. *Nat Rev Gastroenterol Hepatol*. 2020;17:597–617.
13. Parker N, Tsai HH, Ryder SD, Raouf AH, Rhodes JM. Increased rate of sialylation of colonic mucin by cultured ulcerative colitis mucosal explants. *Digestion*. 2009;56:52–56. doi:10.1159/000201222
14. Brazil JC, Parkos CA. Finding the sweet spot: glycosylation mediated regulation of intestinal inflammation. *Mucosal Immunol*. 2022;15:211–222.
15. Fan Q, Dai W, Li M, et al. Inhibition of  $\alpha$ 2,6-sialyltransferase relieves symptoms of ulcerative colitis by regulating Th17 cells polarization. *Int Immunopharmacol*. 2023;125:1–12. doi:10.1016/j.intimp.2023.111130
16. Huang Y-L, Chassard C, Hausmann M, von Itzstein M, Hennot T. Sialic acid catabolism drives intestinal inflammation and microbial dysbiosis in mice. *Nat Commun*. 2015;6:1–11.
17. Fang J, Wang H, Zhou Y, Zhang H, Zhou H, Zhang X. Slimy partners: the mucus barrier and gut microbiome in ulcerative colitis. *Exp Mol Med*. 2021;53:772–787.
18. Ide D, Gorelik A, Illes K, Nagar B. Structural analysis of mammalian sialic acid esterase. *J mol Biol*. 2024;436:1–13.
19. Vos GM, Hooijschuur KC, Li Z, et al. Sialic acid O-acetylation patterns and glycosidic linkage type determination by ion mobility-mass spectrometry. *Nat Commun*. 2023;14:1–13. doi:10.1038/s41467-023-42575-x
20. Sevdali E, Tsitsami E, Tsinti M, et al. SIAE rare variants in juvenile idiopathic arthritis and primary antibody deficiencies. *J Immunol Res*. 2017;2017:1–11. doi:10.1155/2017/1514294
21. Surolija I, Pirnie SP, Chellappa V, et al. Functionally defective germline variants of sialic acid acetyltransferase in autoimmunity. *Nature*. 2010;466:243–247.
22. Corfield AP, Wagner SA, Ljd O, Durdey P, Mountford RA, Clamp JR. The roles of enteric bacterial sialidase, sialateO-acetyl esterase and glycosulfatase in the degradation of human colonic mucin. *Glycoconjugate J*. 1993;10:72–81. doi:10.1007/BF00731190
23. Yang S, Mishra S, Chen L, et al. Integrated glycoprotein immobilization method for glycopeptide and glycan analysis of cardiac hypertrophy. *Anal Chem*. 2015;87:9671–9678. doi:10.1021/acs.analchem.5b01663
24. Yang S, Li Y, Shah P, Zhang H. Glycomic analysis using glycoprotein immobilization for glycan extraction. *Anal Chem*. 2013;85:5555–5561. doi:10.1021/ac400761e
25. Yang S, Hu Y, Sokoll L, Zhang H. Simultaneous quantification of N- and O-glycans using a solid-phase method. *Nat Protoc*. 2017;12:1229–1244. doi:10.1038/nprot.2017.034
26. Yang S, Jankowska E, Kosikova M, Xie H, Cipollo J. Solid-phase chemical modification for sialic acid linkage analysis: application to glycoproteins of host cells used in influenza virus propagation. *Anal Chem*. 2017;89:9508–9517. doi:10.1021/acs.analchem.7b02514
27. Warde-Farley D, Donaldson SL, Comes O, et al. The GeneMANIA prediction server: biological network integration for gene prioritization and predicting gene function. *Nucleic Acids Res*. 2010;38:W214–W220.
28. Yang S, Zhang L, Thomas S, et al. Modification of sialic acids on solid phase: accurate characterization of protein sialylation. *Anal Chem*. 2017;89:6330–6335. doi:10.1021/acs.analchem.7b01048
29. Visser EA, Moons SJ, Spbe T, de Jong H, Boltje TJ, Büll C. Sialic acid O-acetylation: from biosynthesis to roles in health and disease. *J Biol Chem*. 2021;297:100906. doi:10.1016/j.jbc.2021.100906
30. Yao Y, Kim G, Shafer S, et al. Mucus sialylation determines intestinal host-commensal homeostasis. *Cell*. 2022;185:1172–1188.e28. doi:10.1016/j.cell.2022.02.013
31. Ge SX, Jung D, Yao R. ShinyGO: a graphical gene-set enrichment tool for animals and plants. *Bioinformatics*. 2020;36:2628–2629. doi:10.1093/bioinformatics/btz931
32. Yoshida H, Granger ND. Inflammatory bowel disease: a paradigm for the link between coagulation and inflammation. *Inflamm Bowel Dis*. 2009;15:1245–1255. doi:10.1002/ibd.20896
33. Foley JH, Conway EM. Cross talk pathways between coagulation and inflammation. *Circ Res*. 2016;118:1392–1408. doi:10.1161/CIRCRESAHA.116.306853
34. Danese S, de la Motte C, Fiocchi C. Platelets in Inflammatory Bowel Disease: clinical, Pathogenic, and Therapeutic Implications. *Am J Gastroenterol*. 2004;99:938–945. doi:10.1111/j.1572-0241.2004.04129.x
35. Scherlinger M, Richez C, Tsokos GC, Boilard E, Blanco P. The role of platelets in immune-mediated inflammatory diseases. *Nat Rev Immunol*. 2023;23:495–510. doi:10.1038/s41577-023-00834-4
36. Wang H, Kim SJ, Lei Y, et al. Neutrophil extracellular traps in homeostasis and disease. *Sig Transduct Target Ther*. 2024;9:1–40.
37. Hong D, Kim HK, Yang W, et al. Integrative analysis of single-cell RNA-seq and gut microbiome metabarcoding data elucidates macrophage dysfunction in mice with DSS-induced ulcerative colitis. *Commun Biol*. 2024;7:1–14. doi:10.1038/s42003-024-06409-w
38. Gerner RR, Klepsch V, Macheiner S, et al. NAD metabolism fuels human and mouse intestinal inflammation. *Gut*. 2018;67:1813–1823. doi:10.1136/gutjnl-2017-314241
39. Salmenkari H, Korpela R, Vapaatalo H. Renin-angiotensin system in intestinal inflammation - Angiotensin inhibitors to treat inflammatory bowel diseases? *Basic Clin Pharmacol Toxicol*. 2021;129:161–172. doi:10.1111/bcpt.13624
40. Montenegro ML, Corral JE, Lukens FJ, et al. Pancreatic disorders in patients with inflammatory bowel disease. *Dig Dis Sci*. 2022;67:423–436. doi:10.1007/s10620-021-06899-2
41. Fournier B, Philpott Dana J. Recognition of staphylococcus aureus by the innate immune system. *Clin Microbiol Rev*. 2005;18:521–540. doi:10.1128/CMR.18.3.521-540.2005
42. Lin Y, Xiong W, Xiao S, et al. Pharmacoproteomics reveals the mechanism of Chinese dragon's blood in regulating the RSK/TSC2/mTOR/ribosome pathway in alleviation of DSS-induced acute ulcerative colitis. *J Ethnopharmacol*. 2020;263:1–11. doi:10.1016/j.jep.2020.113221

43. Figueiredo VC, Markworth JF, Durainayagam BR, et al. Impaired ribosome biogenesis and skeletal muscle growth in a murine model of inflammatory bowel disease. *Inflamm Bowel Dis*. 2016;22:268–278. doi:10.1097/MIB.0000000000000616
44. Fan W, Ding C, Liu S, et al. Estrogen receptor  $\beta$  activation inhibits colitis by promoting NLRP6-mediated autophagy. *Cell Rep*. 2022;41:1–23. doi:10.1016/j.celrep.2022.111454
45. Grabenstein S, Barnard KN, Anim M, et al. Deacetylated sialic acids modulates immune mediated cytotoxicity via the sialic acid-Siglec pathway. *Glycobiology*. 2021;31:1279–1294. doi:10.1093/glycob/cwab068
46. Corfield AP, Myerscough N, Warren BF, Durdey P, Paraskeva C, Schauer R. Reduction of sialic acid O-acetylation in human colonic mucins in the adenoma-carcinoma sequence. *Glycoconjugate J*. 1999;16:307–317. doi:10.1023/A:1007026314792
47. Kumari R, Majumder MM, Lievonen J, et al. Prognostic significance of esterase gene expression in multiple myeloma. *Br J Cancer*. 2021;124:1428–1436. doi:10.1038/s41416-020-01237-1
48. Mandal C, Schwartz-Albiez R, Vlasak R. Functions and BIOSYNTHESIS of O-Acetylated Sialic Acids. In: Gerardy-Schahn R, Delannoy P, von Itzstein M, editors. *SialoGlyco Chemistry and Biology I: Biosynthesis, Structural Diversity and Sialoglycopathologies*. Berlin, Heidelberg: Springer Berlin Heidelberg; 2015:1–30.
49. Chang -Y-Y, Yu LC-H, Yu IS, et al. Deletion of cadherin-17 enhances intestinal permeability and susceptibility to intestinal tumour formation. *J Pathol*. 2018;246:289–299. doi:10.1002/path.5138
50. Tytgat KM, Opdam FJ, Einerhand AW, Büller HA, Dekker J. MUC2 is the prominent colonic mucin expressed in ulcerative colitis. *Gut*. 1996;38:554–563. doi:10.1136/gut.38.4.554
51. Gruver AM, Westfall MD, Ackermann BL, et al. Proteomic characterisations of ulcerative colitis endoscopic biopsies associate with clinically relevant histological measurements of disease severity. *J Clin Pathol*. 2022;75:636–642. doi:10.1136/jclinpath-2021-207718
52. Woznicki JA, Saini N, Flood P, et al. TNF- $\alpha$  synergises with IFN- $\gamma$  to induce caspase-8-JAK1/2-STAT1-dependent death of intestinal epithelial cells. *Cell Death Dis*. 2021;12:1–15. doi:10.1038/s41419-021-04151-3
53. Li L, Miao X, Ni R, et al. Epithelial-specific ETS-1 (ESE1/ELF3) regulates apoptosis of intestinal epithelial cells in ulcerative colitis via accelerating NF- $\kappa$ B activation. *Immunol Res*. 2015;62:198–212. doi:10.1007/s12026-015-8651-3
54. Fei Y, Liu X-S, Wang F, Wang W, Liu S-L. E-cadherin expression in normal and abnormal tissue specimens from patients with pancreatic carcinoma. *Lab Med*. 2010;41:473–477. doi:10.1309/LMXTBGYUXTVMWS61
55. Lechuga S, Ivanov AI. Disruption of the epithelial barrier during intestinal inflammation: quest for new molecules and mechanisms. *Biochim Biophys Acta*. 2017;1864:1183–1194. doi:10.1016/j.bbamer.2017.03.007
56. Flynn RA, Pedram K, Malaker SA, et al. Small RNAs are modified with N-glycans and displayed on the surface of living cells. *Cell*. 2021;184:3109–3124.e22. doi:10.1016/j.cell.2021.04.023
57. Li J, Yue S, Gao Z, et al. Novel approach to enriching glycosylated RNAs: specific capture of glycoRNAs via solid-phase chemistry. *Anal Chem*. 2023;95:11969–11977. doi:10.1021/acs.analchem.3c01630
58. Azcutia V, Kelm M, Fink D, et al. Sialylation regulates neutrophil transepithelial migration, CD11b/CD18 activation, and intestinal mucosal inflammatory function. *JCI Insight*. 2023;8:1–16. doi:10.1172/jci.insight.167151